High-Resolution, Wide-Field 3D Histopathology for the Morphological Characterization of Prostate Cancer

Andrew Sugarman

November 27, 2023

SPECIFIC AIMS

Abnormal tissue morphology is a hallmark of many soft tissue tumors. Characterization of morphology at the macroscopic or microscopic level can provide insights critical to diagnosis, prognosis, therapeutic design, and even basic research. At the macroscopic level, a variety of three-dimensional imaging technologies (e.g., MRI, CT, and PET-CT) exist and allow clinicians to stage cancer and direct therapies based on the size and shape of lesions [1, 2]. Complementing these imaging technologies, machine learning and statistics advances allow researchers to quantify morphologic characteristics to aid cancer diagnosis and prognosis [3, 4]. Morphology is just as critical at the microscopic level. For example, in prostate cancer, glandular morphology is critical to cancer staging and is the main component of the popular Gleason score [5, 6]. However, at the microscopic level, clinicians and researchers have been limited primarily to qualitative assessment of two-dimensional, slide-based imaging [7]. Assessing morphology in only two dimensions can be sub-optimal [8, 9, 10]. For example, the angle at which a two-dimensional tissue slice is taken can alter conclusions about glandular morphology [11] and is hypothesized to lead to the large variability in prostate cancer grading between observers [11, 12]. In short, there is a dearth of tools available for assessing three-dimensional tissue morphology at the microscopic level.

Recent microfocus Computed Tomography (micro-CT) advances can facilitate high-resolution three-dimensional imaging of biological tissue [13, 14]. In particular, synchrotron micro-CT techniques have demonstrated the ability to resolve cellular structures. However, these methods often require dedicated beamlines or are limited in their field of view [15, 16, 17]. To address this problem, Dr. Cheng's lab has shown how a novel wide-field detector can generate millimeter scale images at sub-micrometer resolution [18]. Recently, we developed a Propagation-Based phase-contrast CT (PBCT) imaging protocol that eliminates the need to stain tissue blocks and thereby permits direct imaging of clinical biopsies, which are often paraffin-embedded and challenging to stain. Using this technology, we have been able to produce the highest-resolution three-dimensional images of prostate cancer and melanoma to date. In what follows, I propose to expand upon this technology and demonstrate its ability as both a clinical and research tool. In Aim 1, we will optimize the PBCT protocol to ease future technology adoption. In Aims 2 and 3, we will evaluate the capabilities of this imaging technology as a clinical and research tool for prostate cancer.

Aim 1: Optimize PBCT imaging of Formalin-Fixed Paraffin-Embeded (FFPE) soft-tissue biopsies. My preliminary results already establish that PBCT is capable of producing high-resolution images of soft-tissue biopsies even in settings where contrast-enhancing staining of tissue blocks is not possible. To optimize this protocol, we will develop a multi-tissue atlas demonstrating how key protocol parameters (e.g., x-ray energy and propagation distance) affect image characteristics including resolution and contrast in different tissue types such as mouse breast cancer, human melanoma, and human prostate cancer. This atlas will assist researchers in determining optimal imaging parameters for their studies.

Aim 2: Evaluate utility of PBCT imaging for the grading of prostate cancer. I will collect the first micro-CT dataset of prostate cancer. Biopsies from disease subjects and age-matched healthy controls will be used to assess the test the hypothesis that PBCT grading is non-inferior to standard slide-based imaging. Beyond this pilot study, these data will be made available publicly as a resource for the community.

Aim 3: Quantify the morphological heterogeneity in prostate glands using computational persistent homology. Computational topology provides a rich suite of tools for quantifying three-dimensional shapes in such a way that morphology can be included as covariates in statistical and machine learning-based cancer prognostics [1, 4]. Under the direction of Dr. Silverman, we will identify which topological summary statistics can best capture the morphologic differences between cancerous and healthy prostate glands. Using these statistics, we will then provide the first quantification of how glandular morphology varies spatially within a biopsy as a function of age and disease status. This quantification will provide novel biological insights into tumor heterogeneity and will inform the design of future studies of prostate cancer.

Completing these aims will provide three critical outcomes: (1) the first micro-CT imaging protocol for the high-resolution 3D imaging of whole tissue blocks, (2) a clinical evaluation of this technology in the context of prostate cancer grading, and (3) the first quantitative study of morphological variation in prostate cancer. Finally, this research will provide me with the skills and expertise to pursue my long-term career goal of leading an independent research program in Oncology.

RESEARCH STRATEGY

Significance

Abnormal morphology is a hallmark of many cancers and is critical in diagnostic, prognostic, and treatment decisions [19]. Both macroscopic morphology (e.g., the shape of a tumor as a whole) and microscopic morphology (e.g., the shape of prostate glands) are clinically important. While clinicians and researchers have numerous tools available for assessing and quantifying morphology at the macroscopic level, comperable tools are often unavailable at the microscopic level. At the macroscopic level, clinicians assess morphology using 3D imaging technologies such as magnetic resonance imaging (MRI) or computed tomography (CT). Yet at the microscopic level, morphological assessment is almost exclusively done by traditional 2D slide-based imaging. Numerous studies have found that 2D imaging can be sub-optimal for assessing cancer morphology [9, 10, 16]. For example, in staging prostate cancer, Koyuncu et al. found that the slice angle used to prepare 2D slides could alter the apparent morphology of glands and alter grading decisions [10]. It is hypothesized that such problems may be partially responsible for the large variability in grading between individuals [8]. Outside of the imaging technologies themselves, the ubiquity of 3D images of cancer have led to numerous statistical and machine learning advances that may ultimate improve clinical care. For example, Crawford et al. showed that computational topology could be used identify the morphological biomarkers for MRI imaging of Glioblastoma that were more predictive of patient outcomes than traditional clinical metrics or even molecular biomarkers [4]. Tools such as those developed by Crawford et al. [4, 3] cannot be applied at the microscopic level due to the lack of 3D imaging data. In short, assessement of cancer morphology is limited at the microscopic level due to a lack of available imaging technologies.

Several approaches to 3D microscopic imaging have recently been proposed. These include the hybrid Open-Top Light-Sheet microscopy (OTLS) illustrated in Glaser et al. [20] and a number of related methods collectively called micro-CT [21, 22, 14, 15, 17]. OTLS is a 3D imaging method that relies on tissue clearing and fluorescent staining of tissue samples. OTLS permits high-quality volumetric imaging of whole biopsies without requiring repeated sectioning. Yet, OTLS requires complicated sample preparation procedures involving tissue clearing and staining with fluorescent markers. Micro-CT however can provide 3D imaging of biological samples at a resolution exceeding OTLS without tissue clearing [16, 22, 23].

While multiple groups have shown that micro-CT is capable of producing high-resolution cellular and sub-cellular imaging, these technologies have been limited by their narrow field-of-view. For example, while Pinkert-Leetsch et al. demonstrated that they could resolve nuclei within pancreatic adenocarcinoma, their entire field of view was only 1.6 by 1.4mm [16]. This is a much more narrow field-of-view than traditional slide-based imaging. My lab recently addressed this issue and desmontrated that a novel wide-field detector allowed for millimeter-scale (whole-biopsy) imaging at sub-micrometer resolution [18].

Contrast-enhancing stains are typically required to obtain high-quality micro-CT images of biological tissue [22, 24, 25, 26]. Yet many clinical samples are Formalin-Fixed and Paraffin-Embedded (FFPE) and do not take up those stains without significant alterations to the sample such as deparaffinization. Recently, Frohn et al., demonstrated that high-resolution stain-free micro-CT of FFPE pancreatic biopsies could be obtained using Propagation-Based phase-contrast CT and phase-retrieval algorithms developed for traditional (macroscopic) CT [27]. In brief, PBCT reconstructs high-resolution 3D images by using the fact that the phase of photons change differently depending on their incident energy and the type of material they pass through. This is in contrast to traditional CT imaging that primarily focuses on the magnitude of attenuation as photons pass through a material [24, 26]. Yet two factors limit the utility of their approach. First, they had the same limited field-of-view typical of micro-CT. Second, their approach a number of non-standard tools as part of the imaging apparatus including Kirkpatrick-Baez (KB) mirrors and a waveguide or an even an interferometer [17, 28, 29].

Recently we have demonstrated that our wide-field detector could be combined with a modified PBCT protocol to obtain high-resolution, whole-biopsy, stain-free micro-CT images of clinical biopsies (Figure 1). Notably, our modified PBCT protocols does not requires the KB mirrors or waveguides and is therefore simpler than some of the prior PBCT protocols with no appreciable decrease in resolution. With this development effective 3D microscopic imaging of clinical biopsies is possible. In the proposed work, we apply this technology to the whole-biopsy imaging of prostate needle-core biopsies. Prostate biopsy imaging is a logical application of our PBCT method, as the diagnosis of prostate cancer relies on the qualitative assessment of glandular shape and arrangement in 2D, which has been known to exhibit a high degree of inter-observer variability[8, 3, 10]. In this proposal, we will demonstrate the ability of high-resolution 3D imaging to fully quantify the shape and shape

variation of healthy and malignant prostate glands.

We first validate this imaging method through a novel non-inferiority trial. 3D imaging is an emerging approach to histopathology, but its effectiveness has yet to be studied in direct comparison to the gold standard. In the proposed work, we will present clinically-trained pathologists with both PBCT and histology images of the same samples and test whether the PBCT images are non-inferior in the grading of prostate cancer. The success of this experiment will motivate larger-scale studies pave the way for the analysis of other tissue types with PBCT.

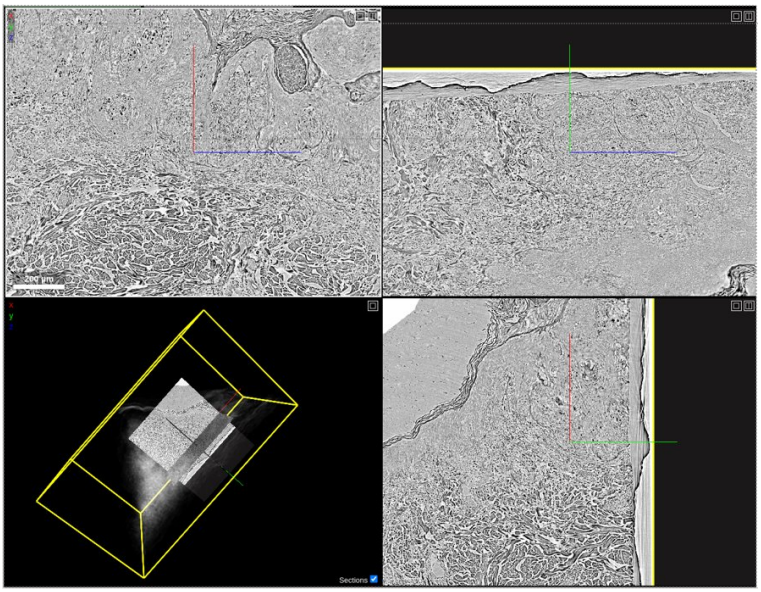

Figure 1: 3-panel view displaying 1 FOV of a PBCT scan of an unstained FFPE melanoma biopsy hosted on the Cheng Lab adaptation of the Neuroglancer web visualization tool[30]. With PBCT and Neuroglancer the user is able to adjust the window level of the image and scroll throughout the 3D volume at 0.5μm steps in each direction.

Motivated by the 3D problem of measuring morphological changes in prostate glands, we also propose a novel approach to the analysis of micro-CT images. Computational persistent homology is a subset of Topological Data Analysis (TDA) that is focused on the measurement of holes and voids in data[31]. Lawson et. al have demonstrated that persistent homology can be applied to identify different Gleason grades from 2D histopathology images of prostate cancer, but because of the limitations of these images they do not derive any quantitative measurement of shape or architecture that can be modeled. We extend these methods into the third dimension by utilizing a Vietoris-rips filtration. We propose to apply the Smooth Euler Characteristic Transform (SECT) pioneered by Crawford et. al to convert filtration results into a continuous random variable that can be used to model the shape and arrangement of prostate glands. We will apply this method to compare the 3D topological features that best separate benign and malignant prostate glands in a first-of-its kind study.

In what follows, we propose to significantly expand on existing literature with experiments guided by our preliminary data. In Aim 1, we propose to optimize our modified PBCT protocol and provide a multi-tissue atlas that researchers can use determine optimal imaging parameter for different tissue types. Aims 2 and 3 then focus on the application of this technology to imaging prostate biopsies. Aim 2 evaluates the utility of this technology in clinical settings while Aim 3 focuses on adapting quantitative tools developed for macroscopic morphometrics to the microscopic domain. Beyond demonstrating the technology, Aims 2 and 3 provide novel insights into prostate cancer. For example, Aim 3 will provide the first quantitative study of how the morphological features distinguishing healthy versus cancerous prostate glands varies spatially within a tumor, between individuals, as a function of age, and as a function of disease status. Among other uses, that analysis can directly inform the design of future studies of prostate cancer as it will directly inform estimates of effect sizes and sampling variability.

Innovation

The proposed work will provide several innovations in the context of 3D microscopic imaging and the study of prostate cancer.

- The modified PBCT protocol optimized in Aim 1 represents the highest-resolution, stain-free approach to 3D imaging of whole-biopsies to date.
- The multi-tissue atlas developed in Aim 1 will be the first resource that researchers can use to guide their own micro-CT imaging studies of human biopsies.
- Aim 2 will develop, and make publicly available, the first 3D microscopic imaging study of prostate cancer.
- Aim 2 will provide the first assessment of the utility of micro-CT in prostate cancer grading.
- Aim 3 will provide the first quantitative study of morphological characteristics of that distinguish healthy from cancerous prostate glands.
- Aim 3 will provide the first quantitative study of how morphological characteristics that distinguish cancer vary spatially within the prostate and as a function of age and disease status.

Approach

Aim 1: Optimize PBCT Imaging of Formalin-Fixed Paraffin-Embeded (FFPE) Soft-Tissue Biopsies.

I have already developed a PBCT protocol that permits high-resolution, stain-free 3D imaging of whole-biopsies (See demonstration in Figure 1). In contrast to standard contrast-based micro-CT, my approach can be applied to FFPE clinical samples without deparaffinization. While I have already optimized this technology for the identification glandular structure in prostate biopsies, further optimization may be needed for different imaging tasks. Broadly, within the merging field of PBCT questions remain about optimal image acquisition parameters such as free space propagation distance (R) and beam energy (K) [32, 16]. There are presently no resources that researchers can use to determine these parameters.

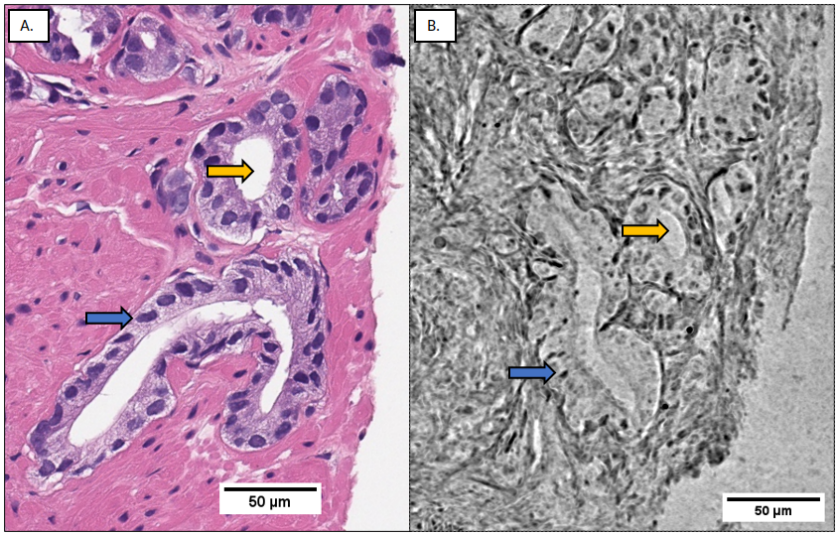

Figure 2: PBCT imaging can resolve glandular structure in prostate biopsies. (A) Histopathology slide taken from a malignant biopsy core, 20X magnification cropped to highlight a section of malignant glands. Nuclei (blue arrow) and lumen (orange arrow) are marked for comparison. (B) 5μm 2D projection of a 3D image obtained from a PBCT scan of the same sample zoomed in to roughly the same region of malignant glands as shown in Panel A. Nuclei (blue arrow) are prominent. The lumina of glands (orange arrow) along with their borders are clearly defined. I obtained this PBCT image at the Lawrence Berkeley National Lab Syncrotron at $K = 20keV$ and $R = 80mm$ without any contrast-enhancing stain. The entire biopsy was imaged, only a small subset of that scan is included for brevity.

The goal of this aim is to provide to provide a publicly available multi-tissue imaging atlas which researchers can use evaluate whether their research question can be answered using PBCT and to determine imaging parameters (R and K) that would best capture the tissue structures of interest. To create this atlas we will image two tumor biopsies and two healthy controls from four distinct tissue types including human prostate cancer, human melanoma, human oropharyngeal cancer, and mouse breast cancer (see letters of collaboration from Drs. Nelson and Hu who will provide samples). For each sample, we will image at a range of distances R from 30mm to 200mm and three different beam energies K (14keV, 20keV, and 70keV). This imaging will be repeated within two different locations to characterize how optimal imaging parameters generalize between laboratories. First, I will image using a bench-top cone-beam source maintained within the Cheng Lab. Second, I will repeat this imaging at the Lawrence Berkeley National Lab (LBNL) syncotron 8.3.2 beamline of the Advanced Light Source (ALS) where Dr. Cheng maintains dedicated time (see letter of support). As these imaging techniques are non-destructive, we will also provide paired slide-based histology images of each sample for comparison. All slide based images, raw scan data, and 3D reconstructions will be made publicly available as an online resource which will allow researchers to determine if their research questions might be studied using PBCT and to quickly identify optimal imaging parameters. Our images will be served online through the open-source web visualization software Neuroglancer [30]. This atlas will be extensible and will serve as a centralized community resource where researcher can share images and the parameter used for imaging.

Potential Pitfalls and Alternative Approaches Overall this aim will be straightforward to complete as I have already established proof-of-concept (e.g., Figures 1 and 2). The major complication that might arise are measurement artifacts called “edge-enhancement” which can occur with propagation-based phase contrast imaging [22, 21]. Notably, these artifacts have been largely absent from our prostate biopsies. That said, if such artifacts are uncounted, we will evaluate different publicly-available phase retrieval algorithms which have been designed for the task [27].

Aim 2: Evaluate Utility of PBCT Imaging For the Grading of Prostate Cancer.

Histopathology of prostate tissue biopsies is the gold standard for the diagnosis and grading of prostate cancer [6]. Grading is based on the Gleason score [8, 6, 12], which typically ranges from 3 to 5 and is primarily defined by glandular morphology within the prostate. However, prior work has shown that Gleason scores can be highly variable both between clinicians and even when the same clinician is shown different slices of the same prostate biopsy [10].This high variability can lead to either under- or over-treatment. It is hypothesized that scoring based

on 3D images may be superior to scoring based on 2D images. Unfortunately, directly testing this hypothesis confronts a form of *familiarity bias* since clinicians trained on traditional slide-based imaging. As a result, here we focus only on a proof of concept focused on testing whether 3D imaging is non-inferior to 2D imaging. To test this hypothesis we will collect, and make available, the first 3D imaging study of prostate cancer.

Develop 3D Imaging Study of Prostate Cancer. In collaboration with Dr. Warrick at PSU we will obtain whole-biopsy PBCT images of 20 age-matched benign and malignant prostate samples (see letter of reference). We will follow the same protocol used for generation of Figure 2B which already established that we can collect high-quality whole-biopsy images of similar biopsies provided by Dr. Warrick. For comparison, after imaging, each sample will be sliced and prepared for slide-based imaging using standard laboratory protocols. To make this data available as a public resource, both the slide-based images as well as the raw and 3D rendered PBCT images will be made available online using the same web-server developed in Aim 1.

Evaluate the Hypothesis That 3D Imaging Can Be Used For Scoring Prostate Cancer. In collaboration with Dr. Warrick, we will recruit up to 10 clinical pathologists (Fellows and Attendings) within and external to PSU to score 3D and 2D images of prostate biopsies. Each pathologist will be asked to provide Gleason scores for each of the prostate biopsies. For each biopsy a pathologist will either be shown the 3D rendering first or the 2D slide-based image first. After providing an initial score, they will then be shown the other imaging type and asked if they need to update their score based on the additional information provided by the second imaging modality. To avoid potential biases, we will randomize the order of samples for each pathologist and for each biopsy randomize whether pathologists are shown the 2D or 3D images first. Ultimately this will result in a two-by-two contingency table Y tabulating the number of individuals shown the 2D or 3D images first and whether or not they found the second imaging modality added information compared to the first. We will test our hypothesis using standard tools from categorical data analysis. We will use a binomial test to evaluate the null hypothesis that the proportion of times where 3D imaging added information to 2D imaging (p_1) is greater than the proportion of times where 2D imaging added information to 3D imaging (p_0). To account for repeated measures we will formulate this test using binomial mixed effects models. To account for familiarity bias we will formulate this as a non-inferiority test with null hypothesis $H_0 : \log p_1/p_0, \leq \delta$ where we will choose $\delta > 0$ rather than $\delta = 0$ to provide a non-inferiority margin. We will chose δ based on the results of a small pilot which will have a simliar design to this one but 2D maximal intensity projectsion (MIPs) from 3D images will be shown rather than full 3D renderings. As in Figure 2, we will show the same region of biopsies using each imaging modality to ensure that the information content between the two imaging types is the same. Participants will be blinded to this fact and therefore we expect that we can estimate $\delta = \log p_1/p_0$ using this pilot study. Note, our sample size is designed to achive $> 85\%$ power under an alternative $\log p_1/p_0 \geq 0.2$ with a non-inferiority margin $\delta \leq -0.2$.

Potential Pitfalls and Alternative Strategies The major limitation we foresee is the complication of *familiarity bias* wherein pathologists will be less likely to find PBCT useful solely because they are unfamiliar with the technology. If our preliminary study estimates $\delta \geq 0.4$, we will compare gray-scale slide-based imaging to PBCT imaging. While standard slide based imaging is often colored, removing this color will likely mitigate the familiarity bias between these two imaging modalities while still allowing for meaningful comparisons.

Aim 3: Quantify the Morphological Heterogeneity in Prostate Glands Using Computational Persistent Homology.

The morphologic features of prostate glands that indicate cancer are abstract and difficult to quantify using standard statistical tool. For example, Figure 3 shows different glandular morphologies associated with different stages of cancer. The differences between Gleason pattern 5 (more diseased) and pattern 1 (healthy) are complex: it is not just a difference in size or volume but a difference of more abstract qualities like “tortuousness”. It is not clear how to quantify these abstract morphologic features let alone how to incorporate some quantitative metric this characteristic into models. Yet, there are numerous potential benefits from quantifying these characteristics. For example, if we could quantify Gleason patterns it provide a more quantitative approach to staging cancer and might improve upon the current Gleason scoring system. Moreover, if we could quantify these characteristics then we use those characteristics in statistical or machine learning models to help predict patient outcomes and guide treatment decisions. In this aim I borrow computational tools developed for macroscopic morphologic analysis of cancer and adapt those tools to the microscopic study of prostate cancer. I then demonstrate those tools by performing the first analysis of morphologic variation within prostate cancer.

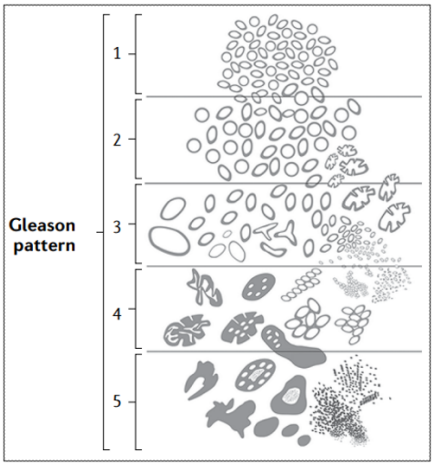

Figure 3: Diagram of different patterns in glandular morphology and the associated Gleason grade. This figure was taken from a review by Rebello et. al [33]

Overview of Computational Persistent Homology Topology is a field of mathematics that, like geometry, studies shapes (See Wasserman et. al [31] for a review on the distinction between these fields). Homology is a subfield of topology that specifically studies the voids or holes in shapes. In the context of prostate cancer, homology can be thought of as the natural field of mathematics for modeling glands which are essentially defined by its void (i.e., lumen). In recent years, homology has moved from an field of abstract math to a powerful framework for modeling shapes thanks to advances in an area of applied statistics called computational persistent homology [31, 34]. In brief, suppose that our shape is defined by a point cloud (e.g., a series 3D points each representing the nucleus of an epithelial cell of a gland). Next pretend that there is a ball of radius r centered about each point. Wherever two balls connect, create an edge between the corresponding points. This forms a graph. Rather than just forming one graph, create a series of graphs as r increases from 0 to infinity. In the language of computational persistent homology this is called a series of simplicial complexes (graphs) formed via a Rips filtration (formed by creating graphs as a function of r). The field of computational persistent homology has created a wide variety of statistics which summarise this series of simplicial complexes in such a way that the resulting statistics capture all the relevant information about homology (points, holes, voids) of the original shape. Those summary statistics can then be used in standard statistical and machine learning models.

Identify Morphologic Features Distinguishing Healthy and Cancerous Prostate Glands In collaboration with Dr. Silverman, I will use 3D renderings of PBCT scans of prostate cancer developed in Aim 2, I will identify morphologic features that distinguish healthy can cancerous prostate glands. Using those scans I will create a labeled dataset of over 100,000 images using standard synthetic-data techniques from computer vision: each rendering will be subset into 500 contiguous, randomly selected sub-regions; each sub-region will be randomly rotated, flipped, and inverted to create up to create no less than 10 synthetic copies of the original sub-region; additional noise will be added to those synthetic copies to ensure robustness of learned morphologic features to measurement noise. Contrast based thresholding of each image will be used to extract point clouds focused on gland cell nuclei. Each point-cloud will then be transformed via the Smooth Euler Characteristic Transform (SECT; which is a statistic calculated from a filtration over the point-cloud) that was recently introduced by Crawford et al. [4] for predicting patient outcomes in Glioblastoma Multiforme from morphologic features in MRI images. Importantly, the SECT maintains information about the homology of the point cloud but transforms that information into the space of smooth functions (into a Sobolev space). This is important as there are numerous statistical and machine learning tools available for modeling such smooth functions.

Using this function representation, I will turn the problem of identifying morphologic features into an equivalent problem of identify a small number of simple functions that can distinguish whether an image came from a cancer or healthy biopsy. More specifically, after turning each synthetic image into a continuous function, those functions will be decomposed into a cubic-spline basis. I will then use standard variable selection techniques from machine learning to identify a small number of components splines that are best able to classify the images. Such tools include penalized regression based methods (e.g., ℓ_1 penalized logistic regression) as well as algorithmic approaches (e.g., forward selection). Standard techniques such as cross validation will be used to help ensure the generalizability of identified morphologic features. Combined with our synthetic data techniques and our use of an age-matched cohort, this approach will ensure that the morphologic features we identify are robust. Ultimately this study will provide a set of morphological features, which can be represented as a low-dimensional (e.g., $<$5 dimensional) vector that provide a concise yet maximally informative representation of the critical morphological characteristics that distinguish healthy versus cancerous prostate tissue.

Characterize Morphologic Variation in Prostate Glands Is the variation in the morphologic features distinguishing cancer greater within a single prostate biopsy or between biopsies? What about variation as a function of age versus variation between health and disease? Answering such questions may provide fundamental insights into the heterogeneity of prostate cancer and are important considerations when designing clinical studies. Yet it has not been possible to directly answer these questions as we have lacked quantifiable morphologic features indicative of prostate cancer. In this sub aim, we use the morphologic features to perform the first quantitative

analysis of morphologic variation in prostate glands and thereby answer such questions.

I will use the results of the prior subaim to calculate, for each position within each 3D rendered PBCT image, the morphologic characteristics distinguishing healthy versus cancerous glandular structure. I will model the resulting data using multivariate mixed-effects models with variance components to identify the relative variation in morphologic structure within a biopsy, between biopsies of age- and disease-matched individuals, between biopsies taken over disease-matched biopsies taken from subjects of different ages, and between age-matched biopsies that differ in disease status. Spatial correlation between morphologic features will be accounted for using first-order conditional-autoregressive variance component. Overall, this will result in a form of multivariate ANOVA: where the relative contributions of different factors (e.g., space, age, disease status) to overall morphologic variation will be quantified.

Potential Pitfalls and Alternative Approaches

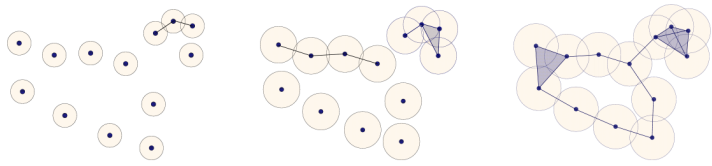

Figure 4: Illustration of a Vietoris-rips complex being formed about a point cloud

Overall the modeling components of this aim are relatively straight forward as the make use of established statistical and machine learning tools that are commonly used within the Silverman lab. The major complication we might encounter is challenges in sampling glandular point-clouds from 3D rendered PBCT images. Based on our preliminary analyses of PBCT imaging of prostate biopsies (e.g., Figure 2) this does not seem likely. Still, it is possible that variation within disease phenotypes such as variation in stromal density or patterns of necrosis may complicate this task. Should we encounter this challenge, we will switch from simple contrast based thresholding to newer deep-learning based image segmentation algorithms (e.g., Ilastik) which I have previously used to segment specific structures in micro-CT images [35]. Once segmented, point-clouds can be generated by uniformly sampling within the segmented gland regions.

Timeline

The proposed aims are synergistic and the success of each aim helps to further subsequent aims. Still, we already have sufficient preliminary data such that the aims can be performed in parallel and the success of each aim is not dependent on previous aims. we have already optimized PBCT for imaging prostate biopsies and therefore Aim 2 can be preformed without Aim 1. Similarly, we already have high-resolution full-biopsy images from a small number of healthy and cancerous prostate biopsies and therefore we can begin preliminary work on Aim 3 even before obtaining the full dataset proposed in Aim 2. Moreover, each aim will correspond to at least one first-author publication. Below we provide a timeline for completion of each subaim.

Aims	Yr1	Yr2	Yr3	Yr4
A1: Perform Imaging for PCBT Atlas				
A1: Develop Neuroglancer Web Interface for Atlas				
A2: Perform PCBT Imaging for Prostate Cancer Study				
A2: Recruit and Survey Clinical Pathologists				
A2: Perform Data Analysis to Test Non-Inferiority				
A3: Develop Quantitative Morphologic Features				
A3: Perform Morphologic Analysis of Variation				

Future Directions

At the completion of this study, we will have developed the first protocol for high-resolution, stain-free, 3D imaging of whole biopsies and we will have evaluated the utility of this technology in the context of prostate-cancer. This work will open up multiple promising avenues for future research, we highlight just three. First, the PBCT imaging protocol we develop and demonstrate in Aim 1 is not limited to prostate cancer. Based on this technology, my approaches to prostate cancer in Aim 2 and 3 could be easily adapted to study other soft-tissue cancers. Second, Aim 2 only serves to evaluate the utility of PBCT imaging in the context of prostate cancer. Should Aim 2 establish that PBCT imaging can be used to grade prostate cancer, future work is needed to more formally study best practices for how to integrate PBCT imaging into clinical-practice. Finally, our analysis of morphologic variation is just one potential use for the morphologic features we develop in Aim 3. Future studies will be needed to evaluating the utility of these features as biomarkers for diagnosis, prognosis, and treatment of disease.

References

[1] S. P. Primakov, A. Ibrahim, J. E. van Timmeren, G. Wu, S. A. Keek, M. Beuque, R. W. Y. Granzier, E. Lavrova, M. Scrivener, S. Sanduleanu, E. Kayan, I. Halilaj, A. Lenaers, J. Wu, R. Monshouwer, X. Geets, H. A. Gietema, L. E. L. Hendriks, O. Morin, A. Jochems, H. C. Woodruff, and P. Lambin, "Automated detection and segmentation of non-small cell lung cancer computed tomography images," Nature Communications, vol. 13, no. 1, p. 3423, Jun. 2022, number: 1 Publisher: Nature Publishing Group. [Online]. Available: https://www.nature.com/articles/s41467-022-30841-3

[2] P. Katiyar, J. Schwenck, L. Frauenfeld, M. R. Divine, V. Agrawal, U. Kohlhofer, S. Gatidis, R. Kontermann, A. Königsrainer, L. Quintanilla-Martinez, C. la Fougère, B. Schölkopf, B. J. Pichler, and J. A. Disselhorst, "Quantification of intratumoural heterogeneity in mice and patients via machine-learning models trained on PET–MRI data," Nature Biomedical Engineering, vol. 7, no. 8, pp. 1014–1027, Aug. 2023, number: 8 Publisher: Nature Publishing Group. [Online]. Available: https://www.nature.com/articles/s41551-023-01047-9

[3] P. Lawson, A. B. Sholl, J. Q. Brown, B. T. Fasy, and C. Wenk, "Persistent Homology for the Quantitative Evaluation of Architectural Features in Prostate Cancer Histology," Scientific Reports, vol. 9, p. 1139, Feb. 2019. [Online]. Available: https://www.ncbi.nlm.nih.gov/pmc/articles/PMC6361896/

[4] L. Crawford, A. Monod, A. X. Chen, S. Mukherjee, and R. Rabadán, "Predicting Clinical Outcomes in Glioblastoma: An Application of Topological and Functional Data Analysis," Journal of the American Statistical Association, vol. 115, no. 531, pp. 1139–1150, Jul. 2020, publisher: Taylor & Francis _eprint: https://doi.org/10.1080/01621459.2019.1671198. [Online]. Available: https://doi.org/10.1080/01621459.2019.1671198

[5] J. Gordetsky and J. Epstein, "Grading of prostatic adenocarcinoma: current state and prognostic implications," Diagnostic Pathology, vol. 11, p. 25, Mar. 2016. [Online]. Available: https://www.ncbi.nlm.nih.gov/pmc/articles/PMC4784293/

[6] J. I. Epstein, "Prostate cancer grading: a decade after the 2005 modified system," Modern Pathology, vol. 31, no. 1, pp. 47–63, Jan. 2018, number: 1 Publisher: Nature Publishing Group. [Online]. Available: https://www.nature.com/articles/modpathol2017133

[7] J. T. C. Liu, A. K. Glaser, K. Bera, L. D. True, N. P. Reder, K. W. Eliceiri, and A. Madabhushi, "Harnessing non-destructive 3D pathology," Nature Biomedical Engineering, vol. 5, no. 3, pp. 203–218, Mar. 2021, number: 3 Publisher: Nature Publishing Group. [Online]. Available: https://www.nature.com/articles/s41551-020-00681-x

[8] T. A. Ozkan, A. T. Eruyar, O. O. Cebeci, O. Memik, L. Ozcan, and I. Kuskonmaz, "Interobserver variability in Gleason histological grading of prostate cancer," Scandinavian Journal of Urology, vol. 50, no. 6, pp. 420–424, Dec. 2016.

[9] W. Xie, N. P. Reder, C. Koyuncu, P. Leo, S. Hawley, H. Huang, C. Mao, N. Postupna, S. Kang, R. Serafin, G. Gao, Q. Han, K. W. Bishop, L. A. Barner, P. Fu, J. L. Wright, C. D. Keene, J. C. Vaughan, A. Janowczyk, A. K. Glaser, A. Madabhushi, L. D. True, and J. T. C. Liu, "Prostate Cancer Risk Stratification via Nondestructive 3D Pathology with Deep Learning-Assisted Gland Analysis," Cancer Research, vol. 82, no. 2, pp. 334–345, Jan. 2022.

[10] C. Koyuncu, A. Janowczyk, X. Farre, T. Pathak, T. Mirtti, P. L. Fernandez, L. Pons, N. P. Reder, R. Serafin, S. S. Chow, V. S. Viswanathan, A. K. Glaser, L. D. True, J. T. Liu, and A. Madabhushi, "Visual assessment of 2D levels within 3D pathology datasets of prostate needle biopsies reveals substantial spatial heterogeneity," Laboratory Investigation; a Journal of Technical Methods and Pathology, p. 100265, Oct. 2023.

[11] R. Serafin, C. Koyuncu, W. Xie, H. Huang, A. K. Glaser, N. P. Reder, A. Janowczyk, L. D. True, A. Madabhushi, and J. T. Liu, "Nondestructive 3D pathology with analysis of nuclear features for prostate cancer risk assessment," The Journal of Pathology, vol. 260, no. 4, pp. 390–401, Aug. 2023.

[12] R. N. Flach, P.-P. M. Willemse, B. B. M. Suelmann, I. A. G. Deckers, T. N. Jonges, C. van Dooijeweert, P. J. van Diest, and R. P. Meijer, "Significant Inter- and Intralaboratory Variation in Gleason Grading of Prostate Cancer: A Nationwide Study of 35,258 Patients in The Netherlands," Cancers, vol. 13, no. 21, p. 5378, Oct. 2021. [Online]. Available: https://www.ncbi.nlm.nih.gov/pmc/articles/PMC8582481/

[13] J. Albers, S. Pacilé, M. A. Markus, M. Wiart, G. Vande Velde, G. Tromba, and C. Dullin, "X-ray-Based 3D Virtual Histology-Adding the Next Dimension to Histological Analysis," Molecular Imaging and Biology, vol. 20, no. 5, pp. 732–741, Oct. 2018.

[14] O. L. Katsamenis, M. Olding, J. A. Warner, D. S. Chatelet, M. G. Jones, G. Sgalla, B. Smit, O. J. Larkin, I. Haig, L. Richeldi, I. Sinclair, P. M. Lackie, and P. Schneider, "X-ray Micro-Computed Tomography for Nondestructive Three-Dimensional (3D) X-ray Histology," The American Journal of Pathology, vol. 189, no. 8, pp. 1608–1620, Aug. 2019. [Online]. Available: https://www.ncbi.nlm.nih.gov/pmc/articles/PMC6680277/

[15] M. Töpperwien, A. Markus, F. Alves, and T. Salditt, "Contrast enhancement for visualizing neuronal cytoarchitecture by propagation-based x-ray phase-contrast tomography," NeuroImage, vol. 199, pp. 70–80, Oct. 2019.

[16] D. Pinkert-Leetsch, J. Frohn, P. Ströbel, F. Alves, T. Salditt, and J. Missbach-Guentner, "Three-dimensional analysis of human pancreatic cancer specimens by phase-contrast based X-ray tomography – the next dimension of diagnosis," Cancer Imaging, vol. 23, no. 1, p. 43, May 2023. [Online]. Available: https://doi.org/10.1186/s40644-023-00559-6

[17] J. Frost, B. Schmitzer, M. Töpperwien, M. Eckermann, J. Franz, C. Stadelmann, and T. Salditt, "3d Virtual Histology Reveals Pathological Alterations of Cerebellar Granule Cells in Multiple Sclerosis," Neuroscience, vol. 520, pp. 18–38, Jun. 2023. [Online]. Available: https://www.sciencedirect.com/science/article/pii/S0306452223001616

[18] M. A. Yakovlev, D. J. Vanselow, M. S. Ngu, C. R. Zaino, S. R. Katz, Y. Ding, D. Parkinson, S. Y. Wang, K. C. Ang, P. La Riviere, and K. C. Cheng, "A wide-field micro-computed tomography detector: micron resolution at half-centimetre scale," Journal of Synchrotron Radiation, vol. 29, no. 2, pp. 505–514, Mar. 2022, number: 2 Publisher: International Union of Crystallography. [Online]. Available: https://journals.iucr.org/s/issues/2022/02/00/mo5248/

[19] e. a. Kumar, Vinay, Robbins Basic Pathology, 10th ed. Elsevier - Health Sciences Division, 2017.

[20] A. K. Glaser, K. W. Bishop, L. A. Barner, E. A. Susaki, S. I. Kubota, G. Gao, R. B. Serafin, P. Balaram, E. Turschak, P. R. Nicovich, H. Lai, L. A. G. Lucas, Y. Yi, E. K. Nichols, H. Huang, N. P. Reder, J. J. Wilson, R. Sivakumar, E. Shamskhou, C. R. Stoltzfus, X. Wei, A. K. Hempton, M. Pende, P. Murawala, H.-U. Dodt, T. Imaizumi, J. Shendure, B. J. Beliveau, M. Y. Gerner, L. Xin, H. Zhao, L. D. True, R. C. Reid, J. Chandrashekar, H. R. Ueda, K. Svoboda, and J. T. C. Liu, "A hybrid open-top light-sheet microscope for versatile multi-scale imaging of cleared tissues," Nature Methods, vol. 19, no. 5, pp. 613–619, May 2022, number: 5 Publisher: Nature Publishing Group. [Online]. Available: https://www.nature.com/articles/s41592-022-01468-5

[21] K. C. Cheng, X. Xin, D. P. Clark, and P. La Riviere, "Whole-animal imaging, gene function, and the Zebrafish Phenome Project," Current Opinion in Genetics & Development, vol. 21, no. 5, pp. 620–629, Oct. 2011.

[22] Y. Ding, D. J. Vanselow, M. A. Yakovlev, S. R. Katz, A. Y. Lin, D. P. Clark, P. Vargas, X. Xin, J. E. Copper, V. A. Canfield, K. C. Ang, Y. Wang, X. Xiao, F. De Carlo, D. B. van Rossum, P. La Riviere, and K. C. Cheng, "Computational 3D histological phenotyping of whole zebrafish by X-ray histotomography," eLife, vol. 8, p. e44898, May 2019, publisher: eLife Sciences Publications, Ltd. [Online]. Available: https://doi.org/10.7554/eLife.44898

[23] M. Töpperwien, F. van der Meer, C. Stadelmann, and T. Salditt, "Correlative x-ray phase-contrast tomography and histology of human brain tissue affected by Alzheimer's disease," NeuroImage, vol. 210, p. 116523, Apr. 2020.

[24] S. R. Katz, M. A. Yakovlev, D. J. Vanselow, Y. Ding, A. Y. Lin, D. Y. Parkinson, Y. Wang, V. A. Canfield, K. C. Ang, and K. C. Cheng, "Whole-organism 3D quantitative characterization of zebrafish melanin by silver deposition micro-CT," eLife, vol. 10, p. e68920, Sep. 2021, publisher: eLife Sciences Publications, Ltd. [Online]. Available: https://doi.org/10.7554/eLife.68920

[25] M. Busse, M. Müller, M. A. Kimm, S. Ferstl, S. Allner, K. Achterhold, J. Herzen, and F. Pfeiffer, "Three-dimensional virtual histology enabled through cytoplasm-specific X-ray stain for microscopic and nanoscopic computed tomography," Proceedings of the National Academy of Sciences, vol. 115, no. 10, pp. 2293–2298, Mar. 2018, publisher: Proceedings of the National Academy of Sciences. [Online]. Available: https://www.pnas.org/doi/abs/10.1073/pnas.1720862115

[26] B. D. Metscher, "MicroCT for comparative morphology: simple staining methods allow high-contrast 3D imaging of diverse non-mineralized animal tissues," BMC Physiology, vol. 9, no. 1, p. 11, Jun. 2009. [Online]. Available: https://doi.org/10.1186/1472-6793-9-11

[27] K. A. Mohan, J.-B. Forien, V. Sridhar, J. A. Cuadra, and D. Parkinson, "Non-Linear Phase-Retrieval Algorithms for X-ray Propagation-Based Phase-Contrast Tomography," Apr. 2023, arXiv:2305.00334 [eess]. [Online]. Available: http://arxiv.org/abs/2305.00334

[28] M. Polikarpov, J. Vila-Comamala, Z. Wang, A. Pereira, S. van Gogh, C. Gasser, K. Jefimovs, L. Romano, Z. Varga, K. Lång, M. Schmeltz, S. Tessarini, M. Rawlik, E. Jermann, S. Lewis, W. Yun, and M. Stampanoni, "Towards virtual histology with X-ray grating interferometry," Scientific Reports, vol. 13, no. 1, p. 9049, Jun. 2023, number: 1 Publisher: Nature Publishing Group. [Online]. Available: https://www.nature.com/articles/s41598-023-35854-6

[29] M. Riedel, K. Taphorn, A. Gustschin, M. Busse, J. U. Hammel, J. Moosmann, F. Beckmann, F. Fischer, P. Thibault, and J. Herzen, "Comparing x-ray phase-contrast imaging using a Talbot array illuminator to propagation-based imaging for non-homogeneous biomedical samples," Scientific Reports, vol. 13, no. 1, p. 6996, Apr. 2023, number: 1 Publisher: Nature Publishing Group. [Online]. Available: https://www.nature.com/articles/s41598-023-33788-7

[30] Google, "Neuroglancer: Web-based volumetric data visualization," 2023. [Online]. Available: https://github.com/google/neuroglancer

[31] L. Wasserman, "Topological Data Analysis," Annual Review of Statistics and Its Application, vol. 5, no. 1, pp. 501–532, 2018, _eprint: https://doi.org/10.1146/annurev-statistics-031017-100045. [Online]. Available: https://doi.org/10.1146/annurev-statistics-031017-100045

[32] C. Norvik, C. K. Westöö, N. Peruzzi, G. Lovric, O. van der Have, R. Mokso, I. Jeremiasen, H. Brunnström, C. Galambos, M. Bech, and K. Tran-Lundmark, "Synchrotron-based phase-contrast micro-CT as a tool for understanding pulmonary vascular pathobiology and the 3-D microanatomy of alveolar capillary dysplasia," American Journal of Physiology-Lung Cellular and Molecular Physiology, vol. 318, no. 1, pp. L65–L75, Jan. 2020, publisher: American Physiological Society. [Online]. Available: https://journals.physiology.org/doi/full/10.1152/ajplung.00103.2019

[33] R. J. Rebello, C. Oing, K. E. Knudsen, S. Loeb, D. C. Johnson, R. E. Reiter, S. Gillessen, T. Van der Kwast, and R. G. Bristow, "Prostate cancer," Nature Reviews Disease Primers, vol. 7, no. 1, pp. 1–27, Feb. 2021, number: 1 Publisher: Nature Publishing Group. [Online]. Available: https://www.nature.com/articles/s41572-020-00243-0

[34] F. Chazal and B. Michel, "An Introduction to Topological Data Analysis: Fundamental and Practical Aspects for Data Scientists," Frontiers in Artificial Intelligence, vol. 4, p. 667963, Sep. 2021. [Online]. Available: https://www.ncbi.nlm.nih.gov/pmc/articles/PMC8511823/

[35] M. A. Yakovlev, K. Liang, C. R. Zaino, D. J. Vanselow, A. L. Sugarman, A. Y. Lin, P. J. L. Riviere, Y. Zheng, J. D. Silverman, J. C. Leichty, S. X. Huang, and K. C. Cheng, "Quantitative Geometric Modeling of Blood Cells from X-ray Histotomograms of Whole Zebrafish Larvae," May 2023, pages: 2023.05.23.541939 Section: New Results. [Online]. Available: https://www.biorxiv.org/content/10.1101/2023.05.23.541939v1